The 4th Joint International Conference on Multibody System Dynamics
May 29 – June 2, 2016, Montréal, Canada

# Mixed Shooting-HBM: a periodic solution solver for unilaterally constrained systems

Frederic Schreyer[1] and Remco I. Leine[1]

[1] *Institute for Nonlinear Mechanics, University of Stuttgart, {schreyer,leine}@inm.uni-stuttgart.de*

ABSTRACT — *In this work, a periodic solution solver for mechanical systems with local nonlinearities is presented. Compared to existing methods, it is especially suitable for nonlinearities which are described by set-valued force laws e.g. set-valued contact laws such as the Signorini condition or impact laws. Such kind of systems are described as differential inclusions or measure differential inclusions and have to be solved using dedicated time integration techniques. The proposed periodic solution solver uses a harmonic ansatz to reduce the dimension of the differential inclusion to enhance the numerical efficiency. Furthermore, for finite element systems a redistributed mass approach is proposed, which generates a massless boundary without changing the global system behavior. The nonlinear problem reduces to a quasi-static equation with inequality complementarity condition and, therefore, can be solved without using time integration techniques. Moreover the Jacobian matrix can be obtained semi-analytically.*

## 1 Introduction

The use of nonlinear Frequency Response Diagrams to avoid nonlinear resonances is becoming ever more important in the design process of machines and mechanical devices. Hereto, periodic solutions of driven mechanical systems with many degrees of freedom need to be calculated in a most efficient way. Mechanical models stemming from industrial applications often consist of very large linear structures (e.g. obtained through a finite element discretization) together with local nonlinearities due to frictional contact. Describing the constraints by set-valued force laws leads to measure differential inclusions which can be simulated within the Nonsmooth Contact Dynamics approach using timestepping methods [1–3].

The most preferred methods to find the periodic steady-state response of nonlinear differential equations are the Harmonic Balance Method (HBM) [4] and the shooting method [5]. The standard HBM approximates the periodic solution in frequency domain and is very popular as it is well suited for large systems with many states. In contrast, the shooting method operates in time domain and relies on numerical time-simulation, making it very versatile as it can also handle nonsmooth dynamical systems. We propose a method which combines the best of both approaches and describes the periodic solution in a mixed frequency time domain, i.e. the Mixed Shooting Harmonic Balance Method (MS-HBM) [6]. It allows to solve the problem on the basis of a differential inclusion with a reduced number of DOF. Hence, the numerically expensive timestepping method needs only to be executed for a system of differential inclusions of reduced dimension. But a disadvantage, compared e.g. to the classical HBM with Alternating Frequency Time Method (AFT) [7], is that the Jacobian matrix must be obtained numerically through finite differences. It makes the method cumbersome for systems with many unilateral constraints such as finite element systems with fine meshes in the contact area. It is known, however, that for such highly discretized systems there is no real need for an impact law as the impact process is sufficiently described by the internal waves within the system. We propose in this paper a modification of the MS-HBM for unilaterally constrained elastic bodies without friction. The mass matrix of the finite element model is redistributed to obtain a massless boundary without changing the global characteristic of the system. Instead of using a differential inclusion, the contact is

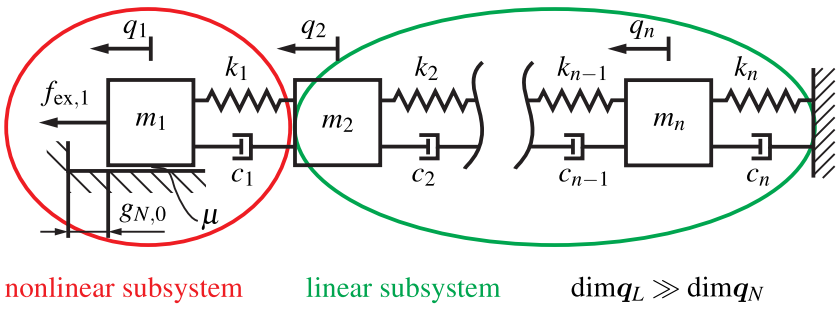


Figure 1: Division into nonlinear and linear subsystems

mathematically described as a quasi-static equation with inequality complementarity condition. The advantage of this approach is that no time integration is necessary and the Jacobian matrix can be obtained semi-analytically.

The paper is organized as follows. Section 2 describes the general MS-HBM. The modification of the MS-HBM using a redistributed mass matrix for finite element models is described in Section 3 for frictionless contact. The approach to obtain the semi-analytical Jacobian matrix is discussed in Section 3.2. The paper closes with a numerical example of a unilaterally constrained bar under harmonic excitation.

## 2 MS-HBM

The mixed shooting-HBM approach exploits the local character of the nonlinearities to find periodic solutions of mechanical systems efficiently. We consider a Lagrangian system of the form

$$\boldsymbol{M}\ddot{\boldsymbol{q}}(t)+\boldsymbol{C}\dot{\boldsymbol{q}}(t)+\boldsymbol{K}\boldsymbol{q}(t)=\boldsymbol{f}_{\mathrm{ex}}(t)+\boldsymbol{f}_{\mathrm{nl}}(t), \tag{1}$$

with the set-valued force law

$$\boldsymbol{f}_{\mathrm{nl}} \in \mathscr{F}_{\mathrm{nl}}(\boldsymbol{q},\dot{\boldsymbol{q}}) \tag{2}$$

where $\boldsymbol{f}_{\mathrm{nl}}$ contains the nonlinear forces which are in the force reservoir $\mathscr{F}_{\mathrm{nl}}(\boldsymbol{q},\dot{\boldsymbol{q}})$ and $\boldsymbol{f}_{\mathrm{ex}}(t)=\boldsymbol{f}_{\mathrm{ex}}(t+T)$ is the periodic forcing. System (1) with set-valued force law (2) constitutes a differential inclusion [1] and, more generally, a measure differential inclusion if (1) is expressed in measures. We assume that the nonlinear forces only act on a subsystem with the generalized coordinates $\boldsymbol{q}_N$ and only depend on $\boldsymbol{q}_N$. The other part of the system, $\boldsymbol{q}_L$, is not directly affected by the nonlinear forces. Therefore, system (1) has the following structure

$$\begin{pmatrix}\boldsymbol{M}_{LL} & \boldsymbol{M}_{LN}\\ \boldsymbol{M}_{NL} & \boldsymbol{M}_{NN}\end{pmatrix}\begin{pmatrix}\ddot{\boldsymbol{q}}_L\\ \ddot{\boldsymbol{q}}_N\end{pmatrix}+\begin{pmatrix}\boldsymbol{C}_{LL} & \boldsymbol{C}_{LN}\\ \boldsymbol{C}_{NL} & \boldsymbol{C}_{NN}\end{pmatrix}\begin{pmatrix}\dot{\boldsymbol{q}}_L\\ \dot{\boldsymbol{q}}_N\end{pmatrix}+\begin{pmatrix}\boldsymbol{K}_{LL} & \boldsymbol{K}_{LN}\\ \boldsymbol{K}_{NL} & \boldsymbol{K}_{NN}\end{pmatrix}\begin{pmatrix}\boldsymbol{q}_L\\ \boldsymbol{q}_N\end{pmatrix}=\begin{pmatrix}\boldsymbol{f}_{\mathrm{ex},L}\\ \boldsymbol{f}_{\mathrm{ex},N}\end{pmatrix}+\begin{pmatrix}\boldsymbol{0}\\ \boldsymbol{f}_N\end{pmatrix}. \tag{3}$$

As an example of such a system, a multi-DOF oscillator with friction, divided into its subsystems, is depicted in Figure 1. The main idea of the MS-HBM is to describe the periodic solution by a combination of frequency and time domain. The dynamics of the linear subsystem is described with its Fourier coefficients $\hat{\boldsymbol{q}}_L$, i.e.

$$\boldsymbol{q}_L(t)=\hat{\boldsymbol{q}}_L^0+\sum_{k=1}^{n_H}\hat{\boldsymbol{q}}_L^{c,k}\cos k\omega t+\hat{\boldsymbol{q}}_L^{s,k}\sin k\omega t=\boldsymbol{V}_+(t)\hat{\boldsymbol{q}}_L, \tag{4}$$

with

$$\boldsymbol{V}_+(t)=\begin{pmatrix}\boldsymbol{I} & \cos(\omega t)\boldsymbol{I} & \sin(\omega t)\boldsymbol{I} & \dots & \cos(n_H\omega t)\boldsymbol{I} & \sin(n_H\omega t)\boldsymbol{I}\end{pmatrix}. \tag{5}$$

The motion $\boldsymbol{q}_L(t)$ of the linear subsystem is therefore constrained to a harmonic oscillation with frequencies $\omega$ up to $n_H\omega$. The nonlinear subsystem is described in time domain and is not constrained to be harmonic. The nonlinear subsystem can be viewed as a non-harmonic forcing on the linear subsystem. The harmonic constraint on the linear subsystem enforces the linear subsystem to oscillate purely harmonically and is therefore a perfect reaction force which balances the higher harmonic components of $\boldsymbol{q}_N$. Consequently, all higher frequencies contained in $\boldsymbol{q}_N$ are

absorbed by the constraint and have no influence on $\boldsymbol{q}_L$. If $\boldsymbol{q}_N$ is known, then $\hat{\boldsymbol{q}}_L$ can be obtained by formulating the first line of Equation 3 in frequency domain which leads to the linear equation

$$\hat{\boldsymbol{q}}_L = \boldsymbol{H}_{LL}^{-1}(\boldsymbol{f}_{\mathrm{ex},L} - \boldsymbol{H}_{LN}\hat{\boldsymbol{q}}_N), \tag{6}$$

where $\boldsymbol{H}_{ij}$ are the dynamic stiffness matrices

$$\boldsymbol{H}_{ij} = \mathrm{diag}(\boldsymbol{J}_{ij,0}, \boldsymbol{J}_{ij,1}, \dots \boldsymbol{J}_{ij,n_H}) \tag{7}$$

with

$$\boldsymbol{J}_{ij,k} = \begin{pmatrix} -\boldsymbol{M}_{ij}(k\omega)^2 + \boldsymbol{K}_{ij} & \boldsymbol{C}_{ij}k\omega \\ -\boldsymbol{C}_{ij}k\omega & -\boldsymbol{M}_{ij}(k\omega)^2 + \boldsymbol{K}_{ij} \end{pmatrix}. \tag{8}$$

The Fourier coefficients of the nonlinear subsystem $\hat{\boldsymbol{q}}_N$ are obtained from $\boldsymbol{q}_N(t)$ through

$$\hat{\boldsymbol{q}}_N = \frac{2}{T}\int_0^T \boldsymbol{V}_-(t)\boldsymbol{q}_N(t)dt, \qquad \boldsymbol{V}_-(t) = \begin{pmatrix} \frac{1}{2}\boldsymbol{I} \\ \cos(\omega t)\boldsymbol{I} \\ \sin(\omega t)\boldsymbol{I} \\ \vdots \\ \cos(n_H\omega t)\boldsymbol{I} \\ \sin(n_H\omega t)\boldsymbol{I} \end{pmatrix}, \tag{9}$$

with $\omega = \frac{2\pi}{T}$ and $n_H$ denoting the number of considered harmonics. The identity matrix $\boldsymbol{I}$ has here the dimension $\dim(\boldsymbol{q}_N)$.

The second line of Equation (3) represents the dynamics of the nonlinear subsystem and therefore remains in time domain. For known $\hat{\boldsymbol{q}}_L$ one can calculate its time domain representation $\boldsymbol{q}_L(t)$ and its derivatives using (4) and solve the differential equation for $\boldsymbol{q}_N(t)$

$$\begin{aligned} &\boldsymbol{M}_{NN}\ddot{\boldsymbol{q}}_N(t) + \boldsymbol{C}_{NN}\dot{\boldsymbol{q}}_N(t) + \boldsymbol{K}_{NN}\boldsymbol{q}_N(t) = -(\boldsymbol{M}_{NL}\ddot{\boldsymbol{V}}_+(t)\hat{\boldsymbol{q}}_L \\ &+ \boldsymbol{C}_{NL}\dot{\boldsymbol{V}}_+(t)\hat{\boldsymbol{q}}_L + \boldsymbol{K}_{NL}\boldsymbol{V}_+(t)\hat{\boldsymbol{q}}_L) + \boldsymbol{f}_{\mathrm{ex},N}(t) + \boldsymbol{f}_N(t) \end{aligned} \tag{10}$$

using numerical time integration techniques. If the nonlinear force $\boldsymbol{f}_N$ is governed by a set-valued force law, then dedicated numerical schemes such as Moreau's timestepping scheme need to be used [1, 2]. A periodic solution can be completely represented by the trajectory $\boldsymbol{q}_N(t)$ on the interval $0 \le t \le T$ and by the Fourier coefficients $\hat{\boldsymbol{q}}_N$ as the Fourier coefficients $\hat{\boldsymbol{q}}_L$ directly follow from $\hat{\boldsymbol{q}}_N$ through (6). The initial condition $\boldsymbol{q}_N(0)$ and $\dot{\boldsymbol{q}}_N(0)$ together with $\boldsymbol{q}_L(t) = \boldsymbol{V}_+(t)\hat{\boldsymbol{q}}_L$ allow to construct $\boldsymbol{q}(t)$ over one period using (10). The vector of unknowns

$$\boldsymbol{x} = \begin{pmatrix} \hat{\boldsymbol{q}}_N \\ \boldsymbol{q}_N(0) \\ \dot{\boldsymbol{q}}_N(0) \end{pmatrix} \tag{11}$$

therefore fully represents a periodic solution of the system. Similar to a shooting method, we require for the nonlinear subsystem the periodicity conditions $\boldsymbol{q}_N(T) - \boldsymbol{q}_N(0) = \boldsymbol{0}$ and $\dot{\boldsymbol{q}}_N(T) - \dot{\boldsymbol{q}}_N(0) = \boldsymbol{0}$, where the state at $t = T$ is obtained through numerical time-integration of (10). The Fourier coefficients $\hat{\boldsymbol{q}}_N$ represent the dynamical behavior of the linear subsystem through (6). To ensure that both subsystems oscillate consistently with each other, the equality $\hat{\boldsymbol{q}}_N - \mathrm{FFT}(\boldsymbol{q}_N(t)) = \boldsymbol{0}$ must hold. In the following, we refer to this equation as connectivity condition. Hence, $\boldsymbol{x}$ represents a periodic solution of the system if it is a zero of the residuum function

$$\boldsymbol{f}_R(\boldsymbol{x}) = \begin{pmatrix} \hat{\boldsymbol{q}}_N - \mathrm{FFT}(\boldsymbol{q}_N(t)) \\ \boldsymbol{q}_N(T) - \boldsymbol{q}_N(0) \\ \dot{\boldsymbol{q}}_N(T) - \dot{\boldsymbol{q}}_N(0) \end{pmatrix}. \tag{12}$$

The problem $\boldsymbol{f}_R(\boldsymbol{x}) = \boldsymbol{0}$ can be solved iteratively using a Newton-type method

$$\boldsymbol{x}^{i+1} = \boldsymbol{x}^i - \left(\frac{\partial \boldsymbol{f}_R}{\partial \boldsymbol{x}}\right)^{-1} \boldsymbol{f}_R(\boldsymbol{x}^i), \tag{13}$$

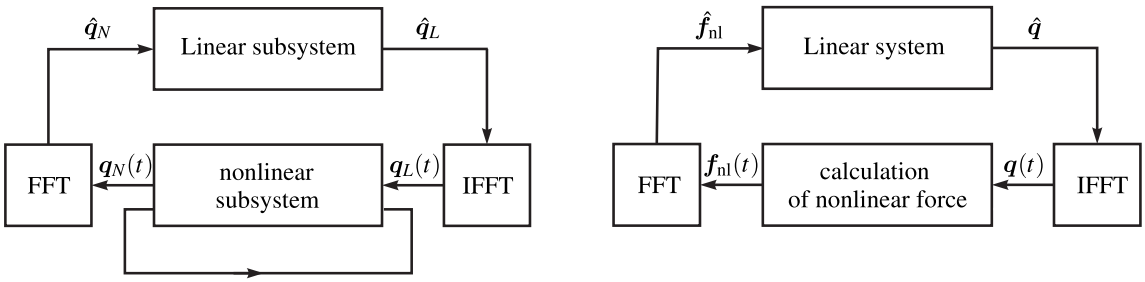


(a) MS-HBM (b) HBM with AFT

Figure 2: Schematic block diagrams

where the Jacobian is obtained through finite differences.

The block diagram of MS-HBM is depicted in Figure 2 and compared to the classical HBM with AFT. The HBM with AFT has a static nonlinearity in the feedback loop and is therefore limited to single-valued force laws, i.e. $\boldsymbol{f}_N$ is a single-valued function of $\boldsymbol{q}_N(t)$. In contrast, the MS-HBM has in the feedback loop a nonlinear dynamical system. This gives the possibility to treat problems with set-valued force laws for which the nonlinear dynamical system in the feedback loop is a (measure) differential inclusion.

The MS-HBM uses time integration techniques and therefore can handle a diversity of problems formulated as differential equations or (measure) differential inclusions [6]. The use of time integration gives the method great generality, but requires a numerical Jacobian calculation. Therefore, the general MS-HBM is numerically not well suited for systems with a large number of DOF of the nonlinear subsystem. Finite element models require in general a fine discretization of the contact zones which directly leads to a large nonlinear subsystem. Therefore, the MS-HBM has its suitability for multi-body systems, but becomes numerically inefficient for elastic bodies. We propose in the following section a modification of the MS-HBM for finite element systems to overcome these problems.

## 3 MS-HBM for finite element systems

We utilize the example system, depicted in Figure 3 to illustrate the benefit of the contact model which is suggested for the modified MS-HBM. The undeformed elastic bar has no internal damping and is accelerated from the rest position under the influence of gravity. The support is considered as rigid. Since no damping is considered, the bar performs a periodic oscillation and the problem can be solved in closed form [8]. The analytical solution is depicted in Figure 4. It shows that after the impact, the bar remains in contact with the support during the time which the shock wave needs to travel up and down the bar. When the bar detaches, it has a uniform velocity and is additionally compressed. Hence, during the flight phase the parabolic motion and the vibration of the bar are superposed. After the second impact and detachment the bar is undeformed again and has a uniform velocity. This sequence is repeated periodically. In the following, we briefly discuss various modeling approaches to describe this system. As first attempt, the problem is modeled as

$$m\ddot{q} = f(q,\dot{q}) + \lambda_N, \tag{14}$$

with a single rigid body using the Signorini condition

$$0 \le g_N \perp \lambda_N \ge 0, \quad g_N = -q + g_{N,0} \tag{15}$$

as contact law. The impact law

$$0 \le \gamma_N^+ + e_N \gamma_N^- \perp \Lambda_N \ge 0 \quad \text{with } 0 \le e_N \le 1 \quad \text{and} \quad \gamma_N = \dot{g}_N \quad a.e., \tag{16}$$

provides a relation between the pre-impact relative velocity $\gamma_N^-$ and the post-impact relative velocity $\gamma_N^+$. Energy conservation is fulfilled for $e_N = 1$ but the contact is never established for a time interval of non-zero size. Contact

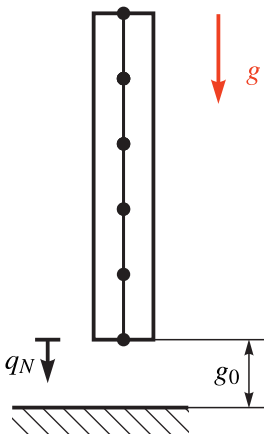


Figure 3: Bar under influence of gravity.

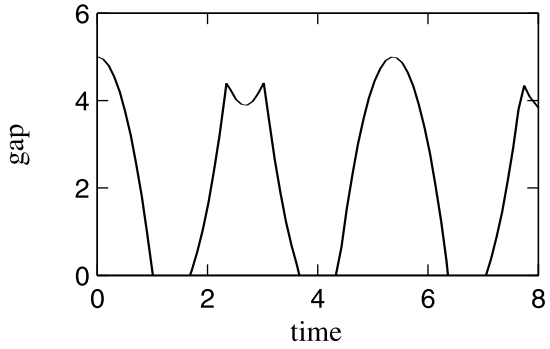


Figure 4: Analytical solution of bar under influence of gravity.

is established for $0 \leq e_N < 1$, possibly after an accumulation point, but energy is not conserved. Obviously, using a rigid body approach one can only describe the global system behavior, but for accurate description of the contact a discretization of the elastic body must be considered. We consider now a Lagrange finite element discretized structure with unilateral constraints

$$\boldsymbol{M}\ddot{\boldsymbol{q}}(t) + \boldsymbol{K}\boldsymbol{q}(t) = \boldsymbol{f}_{\mathrm{ex}}(t) + \boldsymbol{W}_N \boldsymbol{\lambda}_{\mathrm{N}}, \tag{17}$$

and using again the Signorini condition

$$0 \leq \boldsymbol{g}_N \perp \boldsymbol{\lambda}_N \geq 0, \quad \boldsymbol{g}_N = \boldsymbol{W}_N^{\mathrm{T}} \boldsymbol{q} + \boldsymbol{g}_{N,0} \tag{18}$$

as contact law. The hard unilateral constraint demands the implementation of an impact law. Here we use the generalized Newton impact law

$$0 \leq \boldsymbol{\gamma}_N^+ + e_N \boldsymbol{\gamma}_N^- \perp \boldsymbol{\Lambda}_N \geq 0 \quad \text{with } 0 \leq e_N \leq 1 \quad \text{and} \quad \boldsymbol{\gamma}_N = \dot{\boldsymbol{g}}_N \quad a.e., \tag{19}$$

together with the impact equation

$$\boldsymbol{M}(\dot{\boldsymbol{q}}^+ - \dot{\boldsymbol{q}}^-) = \boldsymbol{W}_N \boldsymbol{\Lambda}_N \tag{20}$$

which now provides a relation between the pre- and post-impact relative velocities of the contact node. In the case of a rigid body, the restitution coefficient could be seen as replacement of the internal elastic dynamics. But now, since the bar is modeled as a discretized finite element system, the question of the right restitution coefficient arises. Choosing $e_N = 1$ leads to energy consistency, but the contact is still never established for a time interval of non zero size. Hence, due to the inertia of the other nodes the contact node oscillates during the whole contact period. On the other hand, if $e_N = 0$ the contact is closed for the whole contact time but at each collision of the node, the system loses energy.

Figure 5 shows the gap width and the normalized total energy of the system for each time step. For comparison, the black line represents the analytical solution. It can be seen that, as mentioned before, both choices of the restitution coefficient do not provide the expected result. Therefore, Khenous proposes in [9] to redistribute the mass matrix in order to obtain the desired contact behavior. The massless boundary provides a well-posed problem without the need of an impact law. The $m_{\mathrm{red}}$ curve of Figure 5 shows that this method provides accurate results in time domain calculations, at least for the analyzed example. The increasing deviation with time is mainly due to the finite element discretization (100 elements) which can only approximately model the wave propagation along the bar. In combination with the MS-HBM this redistribution of the mass can provide an accurate and numerically robust approach in frequency domain to calculate periodic solutions which we will show in the following sections.

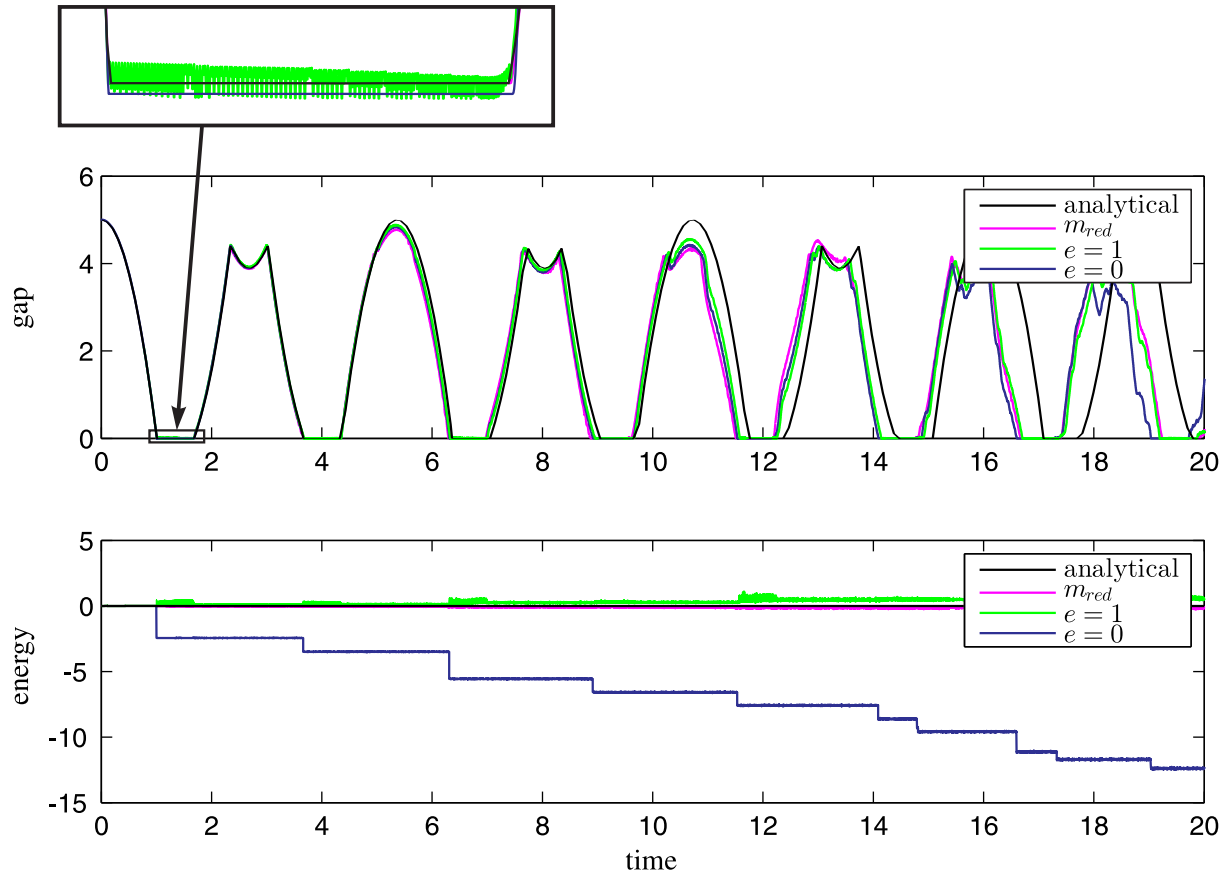


Figure 5: Comparison of different contact descriptions in time domain

To obtain the redistributed mass matrix, we follow the approach proposed in [9]. The idea is to obtain a contact boundary which is massless without changing the global system behavior. The massless contact boundary leads, if we arrange the boundary DOF at the end of the displacement vector, to the new mass matrix

$$\boldsymbol{M}_R = \begin{pmatrix} \bar{\boldsymbol{M}} & \boldsymbol{0} \\ \boldsymbol{0} & \boldsymbol{0} \end{pmatrix}. \tag{21}$$

In [9] $\boldsymbol{M}_R$ is determined through a global minimization problem. The redistributed mass matrix $\boldsymbol{M}_R$ should be as similar to the original mass matrix $\boldsymbol{M}$ as possible which defines the objective function as

$$\Delta M = \frac{1}{2}\|\boldsymbol{M} - \boldsymbol{M}_R\|_{\mathrm{F}}^2, \tag{22}$$

where $\|\boldsymbol{A}\|_{\mathrm{F}} = \sqrt{\mathrm{trace}(\boldsymbol{A}^{\mathrm{T}}\boldsymbol{A})}$ is the Frobenius norm.
Since a Lagrange finite element method is used, the masses are distributed to the nodes in such a way that the zeroth-, first-, and second-order of moments are captured right:

- total mass $\sum_p m_p = \int_\Omega \rho \, \mathrm{d}\Omega$:
- center of gravity $\sum_p x_{i,p} m_p = \int_\Omega \rho x_i \, \mathrm{d}\Omega$:
- moment of inertia $\sum_p x_{i,p} x_{j,p} m_p = \int_\Omega \rho x_i x_j \, \mathrm{d}\Omega$:

Requiring to conserve these conditions during the optimization problem gives the constraint equations. The optimization does neither effect the sparsity nor the symmetry of the mass matrix.

A different approach to obtain a system with massless boundary is proposed in [10]. The creation of the mass matrix with a massless boundary is here directly achieved using new element integration techniques. In this way, the optimization problem of the global mass matrix can be avoided.

### 3.1 MS-HBM with a redistributed mass matrix

The main idea of combining the mass redistribution approach with the MS-HBM is that the nonlinear subsystem then simplifies to a quasi-static system and a time integration becomes obsolete. In the previous section it was shown that the contact for finite element models is still modeled accurately or even better without using an impact law. Moreover, the use of a quasi-static nonlinear subsystem enhances the efficiency of the MS-HBM dramatically. Combining both methods, a general finite element model with local unilateral constraints can then be written as

$$\underbrace{\begin{pmatrix} \bar{\boldsymbol{M}}_{LL} & \boldsymbol{0} \\ \boldsymbol{0} & \boldsymbol{0} \end{pmatrix}}_{\boldsymbol{M}_R} \begin{pmatrix} \ddot{\boldsymbol{q}}_L \\ \ddot{\boldsymbol{q}}_N \end{pmatrix} + \begin{pmatrix} \boldsymbol{K}_{LL} & \boldsymbol{K}_{LN} \\ \boldsymbol{K}_{NL} & \boldsymbol{K}_{NN} \end{pmatrix} \begin{pmatrix} \boldsymbol{q}_L \\ \boldsymbol{q}_N \end{pmatrix} = \begin{pmatrix} \boldsymbol{f}_{\mathrm{ex},L} \\ \boldsymbol{f}_{\mathrm{ex},N} \end{pmatrix} + \begin{pmatrix} \boldsymbol{0} \\ \bar{\boldsymbol{W}}_N \boldsymbol{\lambda}_N \end{pmatrix} \tag{23}$$

with

$$0 \leq \boldsymbol{g}_N \perp \boldsymbol{\lambda}_N \geq 0, \quad \boldsymbol{g}_N = \bar{\boldsymbol{W}}_N^{\mathrm{T}} \boldsymbol{q} + \boldsymbol{g}_{N,0}. \tag{24}$$

We now benefit from the subdivision of the MS-HBM to solve the redistributed problem and obtain a linear equation in frequency domain

$$\hat{\boldsymbol{q}}_L = \boldsymbol{H}_{LL}^{-1} (\hat{\boldsymbol{f}}_{\mathrm{ex},L} - \boldsymbol{H}_{LN} \hat{\boldsymbol{q}}_N), \tag{25}$$

and a nonlinear *static* equation in time domain

$$\boldsymbol{K}_{NN} \boldsymbol{q}_N = -\boldsymbol{K}_{LN} \boldsymbol{q}_L + \bar{\boldsymbol{W}}_N \boldsymbol{\lambda}_N + \boldsymbol{f}_{\mathrm{ex},N} \tag{26}$$

with

$$0 \leq \boldsymbol{g}_N \perp \boldsymbol{\lambda}_N \geq 0, \quad \boldsymbol{g}_N = \bar{\boldsymbol{W}}_N^{\mathrm{T}} \boldsymbol{q} + \boldsymbol{g}_{N,0}. \tag{27}$$

For a given $\hat{\boldsymbol{q}}_N$, Equation (25) directly provides the Fourier coefficients of the linear subsystem $\hat{\boldsymbol{q}}_L$. Hence, the time domain representations of the displacement of the linear part is calculated using the inverse Fourier transformation $\boldsymbol{q}_L = \boldsymbol{V}_+(t) \hat{\boldsymbol{q}}_L$. The dynamics of the nonlinear subsystem (26) with its inequality complementarity condition (27) is reduced to a simple static LCP for each time step instead of a differential inclusion in the case of the general MS-HBM. For each time step $k$ this problem is written using the proximal point equation, which replaces the inequality complementarity condition with an implicit equation for the contact force [2]:

$$\boldsymbol{q}_N^k = \boldsymbol{K}_{NN}^{-1} (-\boldsymbol{K}_{NL} \boldsymbol{q}_L^k + \bar{\boldsymbol{W}}_N \boldsymbol{\lambda}_N^k + \boldsymbol{f}_{\mathrm{ex},N}^k) \tag{28}$$

$$\boldsymbol{\lambda}_N^k = \mathrm{prox}_{\mathbb{R}_0^+} (\boldsymbol{\lambda}_N^k - r(\bar{\boldsymbol{W}}_N^{\mathrm{T}} \boldsymbol{q}_N^k + \boldsymbol{g}_{N,0})) \tag{29}$$

The properties of such quasi-static systems are discussed e.g. in [11]. From the static equation follows directly that $\boldsymbol{q}_N(t)$ describes a periodic but not necessarily a harmonic oscillation. The periodicity condition of Equation (12) becomes therefore unnecessary and thereby the initial condition within the vector of unknowns (11). Thus, we only have to ensure the connectivity condition of both subsystems which defines the residuum function

$$\boldsymbol{f}_R(x) = \hat{\boldsymbol{q}}_N - \mathrm{FFT}(\boldsymbol{q}_N(t)). \tag{30}$$

Correspondingly, the vector of unknowns reduces to

$$\boldsymbol{x} = \hat{\boldsymbol{q}}_N, \tag{31}$$

since the initial conditions are directly given, because $\boldsymbol{q}_N(t)$ is always periodic. This nonlinear equation must again be solved using Newton type methods. But here, the numerically very expensive finite difference method to calculate the Jacobian matrix can be replaced using semi-analytical approaches.

### 3.2 Semi-analytical Jacobian matrix

To gain robustness of the Newton method and to enhance the numerical efficiency a semi-analytical calculation of the Jacobian matrix is proposed. Salles describes in [12] a semi-analytical approach. We derive based on this method a semi-analytical Jacobian calculation for the MS-HBM with redistributed mass matrix. Note, that this is not possible for the general MS-HBM, since the differential inclusion is not differentiable.
With the residuum function (30) and the vector of unknowns (31) the Jacobian matrix is

$$\boldsymbol{J} = \frac{\partial(\hat{\boldsymbol{q}}_N - \mathrm{FFT}(\boldsymbol{q}_N(t)))}{\partial \hat{\boldsymbol{q}}_N} = \boldsymbol{I} - \frac{\partial\,\mathrm{FFT}(\boldsymbol{q}_N(t))}{\partial \hat{\boldsymbol{q}}_N}, \tag{32}$$

where the derivative of the Fourier transformation must be obtained. The Fourier coefficients are defined as the integrals

$$\tilde{\boldsymbol{q}}_N^0 = \frac{2}{T}\sum_{k=1}^{k_\mathrm{end}} \int_{t_k}^{t_k+1} \boldsymbol{q}_N(t)dt \tag{33}$$

$$\tilde{\boldsymbol{q}}_N^{(m,c)} = \frac{2}{T}\sum_{k=1}^{k_\mathrm{end}} \int_{t_k}^{t_k+1} \boldsymbol{q}_N(t)\cos(m\omega t)dt \tag{34}$$

$$\tilde{\boldsymbol{q}}_N^{(m,s)} = \frac{2}{T}\sum_{k=1}^{k_\mathrm{end}} \int_{t_k}^{t_k+1} \boldsymbol{q}_N(t)\sin(m\omega t)dt, \tag{35}$$

where $k$ stands for the different contact states, separation or contact. Using the Leipnitz rule and utilizing that $\boldsymbol{q}_N$ is a continuous and periodic function the derivative of the boundaries $t_k$ and $t_{k+1}$ have no influence on the derivatives of the Fourier transformation. Therefore, $\frac{\partial\,\mathrm{FFT}(\boldsymbol{q}_N)}{\partial \hat{\boldsymbol{q}}_N}$ can be rewritten as

$$\frac{\partial \tilde{\boldsymbol{q}}_N^0}{\partial \hat{\boldsymbol{q}}_N} = \frac{2}{T}\sum_{k=1}^{k_\mathrm{end}} \int_{t_k}^{t_k+1} \frac{\partial \boldsymbol{q}_N(t)}{\partial \hat{\boldsymbol{q}}_N}dt \tag{36}$$

$$\frac{\partial \tilde{\boldsymbol{q}}_N^{(m,c)}}{\partial \hat{\boldsymbol{q}}_N} = \frac{2}{T}\sum_{k=1}^{k_\mathrm{end}} \int_{t_k}^{t_k+1} \frac{\partial \boldsymbol{q}_N(t)}{\partial \hat{\boldsymbol{q}}_N}\cos(m\omega t)dt \tag{37}$$

$$\frac{\partial \tilde{\boldsymbol{q}}_N^{(m,s)}}{\partial \hat{\boldsymbol{q}}_N} = \frac{2}{T}\sum_{k=1}^{k_\mathrm{end}} \int_{t_k}^{t_k+1} \frac{\partial \boldsymbol{q}_N(t)}{\partial \hat{\boldsymbol{q}}_N}\sin(m\omega t)dt. \tag{38}$$

So, the derivative of the FFT boils down to find $\frac{\partial \boldsymbol{q}_N(t)}{\partial \hat{\boldsymbol{q}}_N}$ which can be separated into three steps

$$\frac{\partial \boldsymbol{q}_N(t)}{\partial \hat{\boldsymbol{q}}_N} = \frac{\partial \boldsymbol{q}_N(t)}{\partial \boldsymbol{q}_L(t)} \underbrace{\frac{\partial \boldsymbol{q}_L(t)}{\partial \hat{\boldsymbol{q}}_L}}_{\boldsymbol{V}_+(t)} \underbrace{\frac{\partial \hat{\boldsymbol{q}}_L}{\partial \hat{\boldsymbol{q}}_N}}_{-\boldsymbol{H}_{LL}^{-1}\boldsymbol{H}_{LN}} \tag{39}$$

using the chain rule. The result of the second and third term arise directly from (4) and (25), respectively. To obtain the first term the derivative of the implicit equations (28) and (29) is necessary. The proximal point function can be derived with respect to its argument $z$.

$$\frac{\mathrm{d}\,\mathrm{prox}_{\mathbb{R}_0^+}(z)}{\mathrm{d}z} = \begin{cases} 1 & z > 0 \quad \text{(contact)} \\ 0 & z < 0 \quad \text{(separation)} \\ \emptyset & z = 0 \end{cases} \tag{40}$$

This proximal point equation and its derivative are illustrated in Figure 6. For multiple contact nodes the state of each contact node can be obtained separately. Hence, the derivation of each proximal point function is written as the diagonal matrix

$$\frac{\partial\,\mathrm{prox}(\boldsymbol{z})}{\partial \boldsymbol{z}} = \mathrm{diag}_{i=1\ldots n_{nodes}}\left(\frac{\partial\,\mathrm{prox}(z_i)}{\partial z_i}\right). \tag{41}$$


Figure 6: Derivative of proximal point equation on $\mathbb{R}_0^+$

From Equation (28) one obtains the partial derivative

$$\frac{\partial \boldsymbol{q}_N(t)}{\partial \boldsymbol{q}_L(t)} = \boldsymbol{K}_{NN}^{-1}\left(-\boldsymbol{K}_{NL} + \boldsymbol{W}_N \frac{\partial \boldsymbol{\lambda}_N(t)}{\partial \boldsymbol{q}_L(t)}\right) \tag{42}$$

and with (29)

$$\frac{\partial \boldsymbol{\lambda}_N(t)}{\partial \boldsymbol{q}_L(t)} = \left(\boldsymbol{I} - \frac{\partial\, \mathrm{prox}(\boldsymbol{z})}{\partial \boldsymbol{z}}\left(\boldsymbol{I} - r\boldsymbol{W}_N^{\mathrm{T}}\boldsymbol{K}_{NN}^{-1}\boldsymbol{W}_N\right)\right)^{-1} \frac{\partial\, \mathrm{prox}(\boldsymbol{z})}{\partial \boldsymbol{z}} r\boldsymbol{W}_N^{\mathrm{T}}\boldsymbol{K}_{NN}^{-1}K_{NL}. \tag{43}$$

Finally, the required derivative $\frac{\partial \boldsymbol{q}_N(t)}{\partial \hat{\boldsymbol{q}}_N}$ arises from equation (39). The complete Jacobian entries

$$\boldsymbol{J} = \frac{\partial(\mathrm{FFT}(\boldsymbol{q}_N(t)) - \hat{\boldsymbol{q}_N})}{\partial \hat{\boldsymbol{q}}_N} = \begin{pmatrix} \frac{2}{T}\int_0^{\mathrm{T}} \frac{\partial \boldsymbol{q}_N(t)}{\partial \hat{\boldsymbol{q}}_{N,0}} dt & \frac{2}{T}\int_0^{\mathrm{T}} \frac{\partial \boldsymbol{q}_N(t)}{\partial \hat{\boldsymbol{q}}_{N,1}} dt & \dots \\ \frac{2}{T}\int_0^{\mathrm{T}} \frac{\partial \boldsymbol{q}_N(t)}{\partial \hat{\boldsymbol{q}}_{N,0}} \cos(\omega t) dt & \frac{2}{T}\int_0^{\mathrm{T}} \frac{\partial \boldsymbol{q}_N(t)}{\partial \hat{\boldsymbol{q}}_{N,1}} \cos(\omega t) dt & \dots \\ \frac{2}{T}\int_0^{\mathrm{T}} \frac{\partial \boldsymbol{q}_N(t)}{\partial \hat{\boldsymbol{q}}_{N,0}} \sin(\omega t) dt & \ddots & \vdots \\ \frac{2}{T}\int_0^{\mathrm{T}} \frac{\partial \boldsymbol{q}_N(t)}{\partial \hat{\boldsymbol{q}}_{N,0}} \cos(2\omega t) dt & \dots & \\ \vdots & \dots & \end{pmatrix} \tag{44}$$

are calculated using the Fourier transformation of the derivative for all considered harmonic oscillations. Note that to obtain the Jacobian matrix semi-analytically the inverse matrix $(\boldsymbol{W}_N^{\mathrm{T}}\boldsymbol{K}_{NN}^{-1}\boldsymbol{W}_N)^{-1}$ must exist. This matrix can be seen as the equivalent to the well known Delassus-matrix of nonsmooth systems. Therefore, the regularity of $\boldsymbol{W}_N^{\mathrm{T}}\boldsymbol{K}_{NN}^{-1}\boldsymbol{W}_N$ can be proved in the same way, i.e. $\boldsymbol{W}_N$ needs to have full rank and $\boldsymbol{K}_{NN}$ needs to be invertible.

### 3.3 Numerical examples

As numerical example we use a one-sided clamped bar with a unilateral constraint at the end. It is excited with a harmonic force at the middle of the bar and is discretized with 100 bar elements which have the mass and stiffness matrix

$$\boldsymbol{M}_{\mathrm{e}} = \frac{\rho A l}{6}\begin{pmatrix} 2 & 1 \\ 1 & 2 \end{pmatrix}, \quad \boldsymbol{K}_{\mathrm{e}} = \frac{EA}{l}\begin{pmatrix} 1 & -1 \\ -1 & 1 \end{pmatrix}. \tag{45}$$

Table 1: Selected parameters of the bar.

| parameter | $\rho$ | $E$ | $A$ | $\ell$ | $n_{\mathrm{e}}$ | $\hat{F}$ |
|---|---|---|---|---|---|---|
| value | $9e^{-9}$ | $21e^4$ | 1 | 20 | 100 | 4000 |

The initial gap size is defined as $g_{N,0}$ and the displacement of the contact node is given as $q_N$, see Figure 7. For simplicity a one-dimensional problem is chosen, but the method can easily be used for general finite element

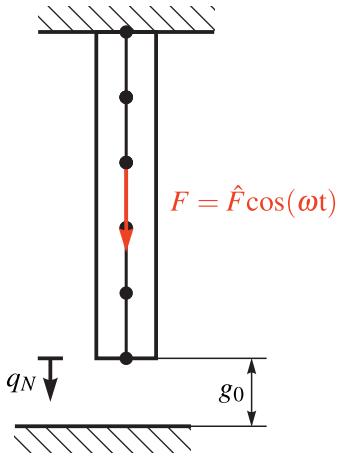


Figure 7: Clamped bar with harmonic excitation.

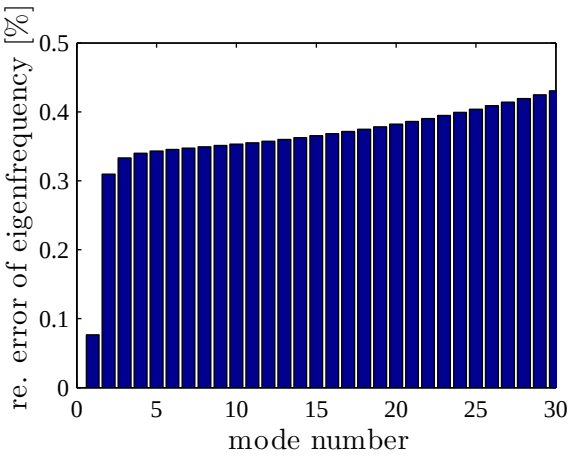


Figure 8: Relative error of eigenfrequencies.

models. The first eigenfrequency of the bar is located at $60335Hz$. To analyze the influence of the mass redistribution on the Frequency Response Diagram the relative error of the first 30 eigenfrequencies are plotted in Figure 8. However, the shift of the eigenfrequencies is negligible.

We first analyze the convergence properties of the MS-HBM with redistributed mass under increasing the number of considered harmonic oscillations. As reference, the steady state solution obtained using time integration technique with the original mass matrix and a restitution coefficient $e_N = 0$ is taken. Figure 9 shows the Frequency Response Diagram of the contact node for the system with an initial gap size of $g_{N,0} = 0.2$. For frequencies far away from the resonance the amplitude of $q_N$ is too small to reach the support, resulting in a linear response of the system. Therefore, the MS-HBM is exact for this frequency range. At frequencies near the first eigenfrequency the bar hits the ground and higher harmonic oscillations have an increasing contribution to the periodic solution. However, with just a few harmonics the MS-HBM provides a very accurate approximation of the FRF. The displacement over time of the periodic solution at $0.06MHz$ is depicted in Figure 10. Even for the weakest approximation with just one harmonic oscillation the nonpenetration condition is fulfilled exactly. The HBM with AFT can only approximately satisfy these contact conditions.

The MS-HBM with redistributed mass has some more advantages compared to the HBM with AFT. It does not need to have a penalty factor which influences the numerical results. In Figure 11 the FRF of the system with the initial gap size $g_{N,0} = 0$ using MS-HBM is compared to the HBM with AFT with different penalty factors $k_p$. Although, with increasing $k_p$ it converges to the MS-HBM and to the solution obtained using time integration, the numerical convergence properties of the Newton method become more and more cumbersome.

## 4 Conclusions and outlook

We present in this paper a MS-HBM which exploits the local character of the nonlinearities of the structure. It calculates the periodic solutions efficiently using a mixed frequency time domain approach. The general MS-HBM is suitable for rigid body systems with many states, since measure differential inclusions can be solved with a reduced number of states. For elastic problems which require often a fine contact discretization at the contact area, this method is limited due to the numerical expensive time integration and the numerically obtained Jacobian matrix. Therefore, the MS-HBM is extended by a redistribution of the mass matrix. It provides the possibility to calculate periodic solutions of finite element systems with frictionless contact very efficiently. We have shown that the method provides accurate results with just a few considered harmonic oscillations. In comparison to HBM with AFT it has no design parameter which has an influence on the result. Further research will focus on stability analysis and add the possibility of frictional contact into the existing MS-HBM with redistributed mass matrix.

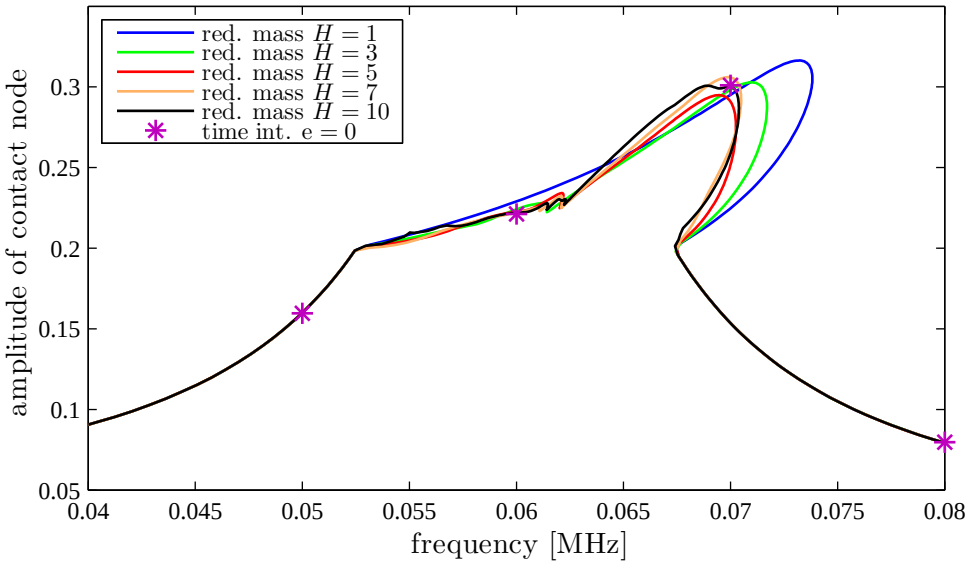


Figure 9: Frequency Response Diagram of clamped bar with an initial gap size $g_{N,0} = 0.2$.

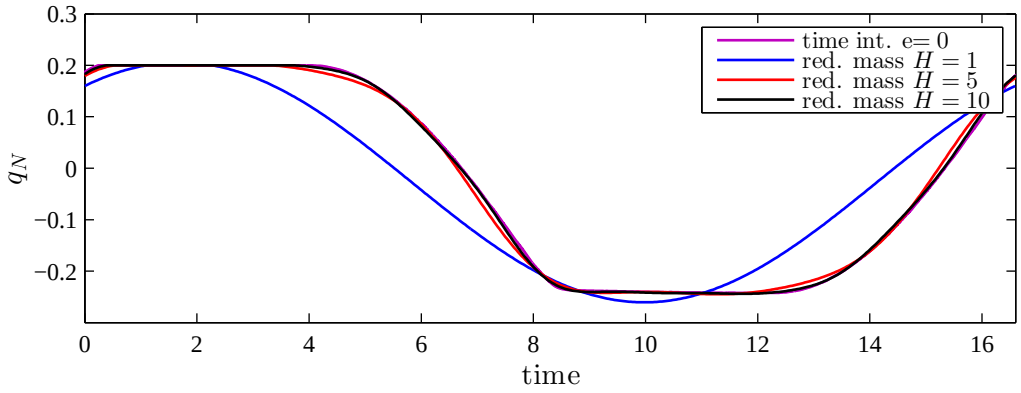


Figure 10: Periodic solution of contact node at 0.06Mhz with an initial gap size $g_{N,0} = 0.2$.

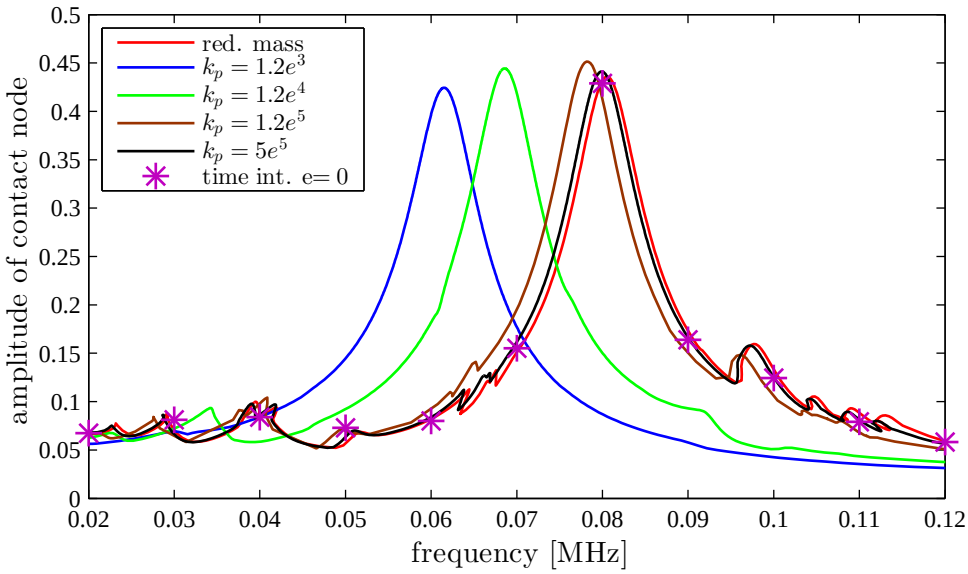


Figure 11: Frequency Response Diagram of clamped bar with 5 considered harmonic oscillations and an initial gap size $g_{N,0} = 0$.

# References


[1] R. I. Leine and H. Nijmeijer, *Dynamics and Bifurcations of Non-smooth Mechanical Systems*, vol. 18 of *Lecture Notes in Applied and Computational Mechanics*. Springer, Berlin, 2004.

[2] V. Acary and B. Brogliato, *Numerical Methods for Nonsmooth Dynamical Systems: Applications in Mechanics and Electronics*, vol. 35 of *Lecture Notes in Applied and Computational Mechanics*. Springer Science & Business Media, Heidelberg, 2008.

[3] C. Studer, R. Leine, and C. Glocker, "Step size adjustment and extrapolation for time-stepping schemes in non-smooth dynamics," *International Journal for Numerical Methods in Engineering*, vol. 76, no. 11, pp. 1747–1781, 2008.

[4] A. H. Nayfeh and D. T. Mook, *Nonlinear Oscillations*. Wiley, New York, 1979.

[5] U. M. Ascher, R. M. Mattheij, and R. D. Russell, *Numerical Solution of Boundary Value Problems for Ordinary Differential Equations*, vol. 13 of *Classics in Applied Mathematics*. SIAM, Philadelphia, 1994.

[6] F. Schreyer and R. I. Leine, "A mixed shooting and harmonic balance method for mechanical systems with dry friction or other local nonlinearities," *Proc. IDETC/CIE*, 2015.

[7] T. Cameron and J. Griffin, "An alternating frequency/time domain method for calculating the steady-state response of nonlinear dynamic systems," *Journal of Applied Mechanics*, vol. 56, no. 1, pp. 149–154, 1989.

[8] D. Doyen, A. Ern, and S. Piperno, "Time-integration schemes for the finite element dynamic Signorini problem," *SIAM Journal on Scientific Computing*, vol. 33, no. 1, pp. 223–249, 2011.

[9] H. B. Khenous, P. Laborde, and Y. Renard, "Mass redistribution method for finite element contact problems in elastodynamics," *European Journal of Mechanics-A/Solids*, vol. 27, no. 5, pp. 918–932, 2008.

[10] C. Hager, S. Hüeber, and B. Wohlmuth, "A stable energy-conserving approach for frictional contact problems based on quadrature formulas," *International Journal for Numerical Methods in Engineering*, vol. 73, no. 2, pp. 205–225, 2008.

[11] A. Klarbring, "Contact, friction and discrete mechanical structures. Analogies and dynamic problems," in *Multibody Dynamics with Unilateral Contacts (CISM Courses and Lectures no 421)*, pp. 147–174, F. Pfeiffer and C Clocker, 2000.

[12] L. Salles, L. Blanc, F. Thouverez, A. M. Gouskov, and P. Jean, "Dynamic analysis of a bladed disk with friction and fretting-wear in blade attachments," in *ASME Turbo Expo 2009: Power for Land, Sea, and Air*, pp. 465–476, American Society of Mechanical Engineers, 2009.